Macromolecules
ARTICLE

Macromolecules **2009**, *42*, 6799–6807 **6799**
DOI: 10.1021/ma900974b

Molecular Dynamics of PEG−Dendrimer Blends and PEGylated Dendrimers

Sanja Natali and Jovan Mijovic*

Othmer-Jacobs Department of Chemical and Biological Engineering, Polytechnic Institute of New York University, Six MetroTech Center, Brooklyn, New York 11201

Received May 4, 2009; Revised Manuscript Received June 24, 2009

ABSTRACT: Molecular dynamics of a series of poly(ethylene glycol)−poly(amidoamine) (PEG−PAMAM) dendrimer blends and PEG conjugated PAMAM dendrimers were investigated and contrasted using broadband dielectric relaxation spectroscopy (DRS). The study was carried with 2000 Da PEG and generation 3 PAMAM dendrimers. The results were generated over a wide range of frequencies and temperatures. A number of relaxation processes were detected and their origin and characteristics established. PEG−dendrimer blends show three local processes and a segmental process contributed by the amorphous PEG. The time scale of segmental relaxation decreases with increasing concentration of dendrimers due to the H-bonding that forms between the PEG oxygen and the amino groups on the surface of dendrimers. PEGylated dendrimers show two local processes and a segmental process, also contributed by the amorphous PEG. But unlike the blends, the amorphous PEG in PEGylated dendrimers is constrained not only by the crystalline lamellae but also by the covalent bonds with the dendrimer. This results in a different morphology which, in turn, gives rise to a different time scale of segmental relaxation in PEG−dendrimer blends and PEGylated dendrimers. A comprehensive analysis of the effect of morphology, concentration of dendrimers, number of attached PEG chains, and temperature on the relaxation time, dielectric relaxation strength, and spectral characteristics of various relaxation processes is offered. The results reported here are expected to provide an added dimension to our understanding of the principles that guide drug delivery concepts.

Introduction

Different types of polymers (linear, cross-linked, and branched) have been used for the design of controlled drug delivery systems.[1−4] Among those, dendrimers stand out as particularly promising nanocarriers for drug and gene delivery.[5−11] A comprehensive overview of nanoparticulates as drug carriers can be found in a recently published book.[12] Dendrimers offer advantages over other polymers architectures in that they have well-defined, compartmentalized structure in the nanometer size range, narrow polydispersity, and globular morphology. Those features enable them to encapsulate molecules such as therapeutic drugs within the interstitial space of their branches for subsequent targeted delivery.[13−15] Poly(amidoamine) (PAMAM) dendrimers are especially attractive for biopharmaceutical applications because they represent the only class of dendrimers that are monodispersed.[16] Most recently, they were shown to be promising candidates as efficient DNA delivery systems.[17] However, for *in vivo* applications a carrier also needs to be nontoxic and nonimmunogenic and to have long circulation time. While cytotoxicity of dendrimers was shown to be generation dependent, with lower generations being less toxic,[18,19] studies on generations 3−7 of amino-terminated PAMAM dendrimers showed that immunogenicity was reduced when poly(ethylene glycol) (PEG) was covalently attached to dendrimers.[20] Further, it was found that by attaching biocompatible PEG to the dendrimer surface, water solubility, lifetime in the bloodstream, and drug loading capacity increase[11] while the rate of drug release decreases.[21] To understand and assess drug loading and releasing capabilities and to usher the way for their optimization, it is important to acquire a comprehensive knowledge of the dynamics of PEGylated dendrimers on the molecular level. Dynamics describe molecular motions with a wide range of length scales and time scales that are affected by molecular weight, structure, surface coverage, chain conformation, and morphology. These are important parameters in drug delivery systems as they control the circulation time, rheological behavior, and release kinetics.

Notwithstanding the extensive amount of research on PEGylated dendrimers, published reports on their dynamics are scarce. In this work we employ dielectric relaxation spectroscopy (DRS) to study dynamics of PEGylated dendrimers. The great advantage of DRS in the study of molecular dynamics lies in its ability to cover a broad range of frequencies (up to 16 decades) and temperature that is not available with other spectroscopic, scattering, or relaxation methods.[22−24]

The principal objective of this study is to conduct a comparative investigation of PEG−dendrimer blends and PEGylated dendrimers by DRS, evaluate the effect of dendrimer concentration and number of attached PEG chains, and quantify the effect of molecular and external factors on dynamics. To the best of our knowledge, this study marks the first published report on the dynamics of PEGylated dendrimers as studied by DRS.

Experimental Section

Materials. *Dendrimers.* Generation 3 poly(amidoamine) (PAMAM) dendrimer with ethylenediamine core and amino surface groups in methanol solution (20 wt %) was obtained from Aldrich.

*Corresponding author: Tel 1 718 2603097; fax 1 718 2603125; e-mail jmijovic@poly.edu.

Published on Web 08/06/2009

Table 1. Investigated Samples

description	wt % of dendrimers	code	T_m (K)	X_c (%)
PEG (hydroxyl end group) + D	5	PEG-D5%	326	78
PEG (hydroxyl end group) + D	10	PEG-D10%	324	66
PEG (hydroxyl end group) + D	18	PEG-D18%	323	55
PEG (epoxy end group) + D	30	PEGylated-8	322	37
PEG (epoxy end group) + D	18	PEGylated-16	323	48
PEG (epoxy end group) + D	10	PEGylated-32	326	61

PEG. Two samples of poly(ethylene glycol) (PEG) with different end groups, one nonreactive (hydroxyl groups on both sides) and the other reactive (epoxy group on the one side and methyl group on the other side), were obtained from Aldrich and SunBio, Inc., respectively. Both PEG samples have the molecular weight of 2000 Da.

PEG−Dendrimer Blends. Blends were prepared by mixing the desired amounts of dendrimer and PEG with nonreactive end groups (hydroxyl) in methanol using a high-speed stirrer. Samples were then placed in a vacuum oven for 7 days in order to remove the solvent completely. In the sample code for blends, the symbol D stands for dendrimer and the number that follows describes the weight percent of dendrimer in the blend. For example, PEG- D5% represents a blend of PEG with 5 wt % of dendrimer.

PEGylated Dendrimers. PEGylated dendrimers were synthesized by adding various amounts of PEG with reactive end group (epoxy) to a solution of dendrimers in methanol. Three molar ratios of PEG to dendrimer were used: 32:1, 16:1, and 8:1. The mixtures were stirred for 24 h at room temperature, using a high-speed stirrer. The solutions were then placed in a vacuum oven for 7 days at 80 °C. The completion of reactions was confirmed by near-infrared (NIR) spectroscopy. The reaction was considered complete when no peak was detected at the epoxy absorption frequency (4520 cm^{-1}). In the sample codes for PEGylated dendrimers (PEGylated-*x*), *x* at the end represents the average number of the attached PEG chains. All investigated systems and their codes are summarized in Table 1. This table also contains the melting temperature and degree of crystallinity obtained by DSC.

Techniques. *Dielectric Relaxation Spectroscopy* (*DRS*). Dielectric measurements were performed in the frequency range from 10^{-1} to 10^{6} Hz using a Novocontrol α Analyzer, which was interfaced to computers and connected to a heating/cooling unit (modified Novocontrol Novocool System) that can control temperature from 173 to 523 K with a precision of ±0.5 K. Samples were placed between two aluminum electrodes, 12 mm in diameter and with 50 μm spacing between them. Further details about our experimental facility for dielectric measurements are given elsewhere.[25]

Differential Scanning Calorimetry (*DSC*). The melting temperature and the degree of crystallinity were determined by DSC using TA Instrument Co. modulated DSC model Q2000. The samples were cooled at 193 K and then heated at 10 K/min to 373 K.

Fourier Transform Infrared Spectroscopy (*FTIR*). FTIR spectroscopy was performed using a Nicolet Magna-IR system 750 spectrometer with spectral range coverage from 15 800 to 50 cm^{-1} and the Vectra interferometer with resolution better than 0.1 cm^{-1}. Near-infrared (NIR) data were obtained using a calcium fluoride beam splitter, a white light source, and a mercury−cadmium−tellurium (MCT) detector. The details of this technique can be found elsewhere.[26]

Results and Discussion

This paper is organized as follows: We begin our discussion by examining the relaxation dynamics of the individual components, generation 3 PAMAM dendrimers, and poly(ethylene glycol), PEG. We then proceed with the analysis of a series of their blends and finish with the discussion of dynamics of PEGylated dendrimers.

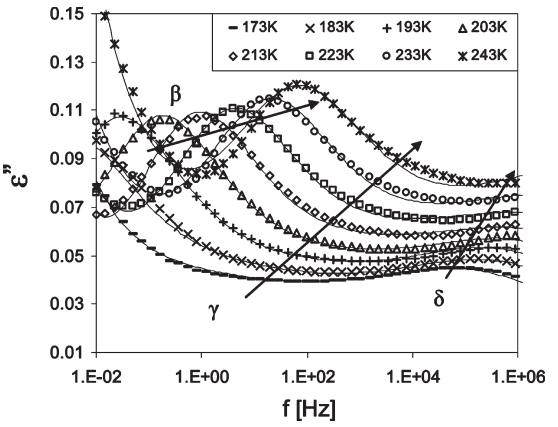

Figure 1. Dielectric loss of dendrimer in the frequency domain with temperature as a parameter.

1. Individual Components. *A. Generation 3 PAMAM Dendrimer*. Dielectric properties of the first six generations of PAMAM dendrimers have been described in our recent publication.[27,28] A brief recap is warranted to facilitate the understanding of dynamics of PEG−dendrimer blends and PEGylated dendrimers. The DSC glass transition temperature of the generation 3 PAMAM dendrimer (hereafter referred to as dendrimer) is 245 K. Dielectric loss in the frequency domain below 245 K with temperature as a parameter is shown in Figure 1. The solid lines in the figure are the combined fits of the sum of ionic conductivity and the Havriliak−Negami (HN) functional form:[29]

$$\varepsilon^*(\omega) = \varepsilon' - i\varepsilon'' = -i\left(\frac{\sigma_c}{\varepsilon_0\omega}\right)^N + \sum_{k=1}^{n}\left[\frac{\Delta\varepsilon_k}{(1+(i\omega\tau_k)^{a_k})^{b_k}} + \varepsilon_{\infty k}\right] \quad (1)$$

where ε_0 is the vacuum permittivity, *N* is the exponent of the frequency-dependent conductivity of ε'', σ_c is the conductivity, *a* and *b* are the shape parameters that define the breadth and the symmetry of the spectrum, respectively, and τ is the average relaxation time.

Dendrimer exhibits three relaxations below the calorimetric T_g. They are labeled β, γ, and δ in the order of increasing frequency at a constant temperature, and their locations are indicated with arrows in Figure 1. These processes shift to higher frequency and increase in intensity with increasing temperature. They are also characterized by the Cole−Cole[30] type relaxation spectra and an Arrhenius-like temperature dependence of the average relaxation time. The corresponding activation energies are summarized in Table 2. The origin of the β process lies in the motions of branch ends that include amino groups. The γ process is affected by the interplay between molecular architecture and hydrogen bonding and is attributed to the motions of the amide groups that are not hydrogen bonded to the neighboring chains. Two types of hydrogen bonding occur in dendrimers: intermolecular (between amide groups on two

Table 2. Activation Energy for Local Processes

	E_a (kJ/mol)		
code	β	γ	Δ
D	61.5	58.2	23.4
PEG-D18%	68.0	58.2	22.4
PEG-D10%	73.1	58.2	23.0
PEG-D5%	90.8	58.2	24.0
PEG			22.5
PEGylated-8	34.9		32.7
PEGylated-16	36.4		30.1
PEGylated-32	34.3		31.3

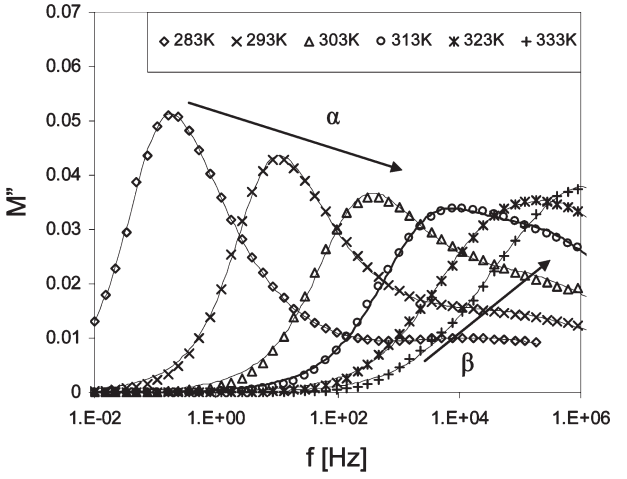

Figure 2. Dielectric loss modulus of dendrimer in the frequency domain with temperature as a parameter.

different molecules) and intramolecular (between amide groups on two different branches of the same dendrimer). The δ process is assigned to the local fluctuations of amino groups on the dendrimer surface.

In the region above the calorimetric T_g, where the segmental process is active, dielectric spectra of dendrimers are dominated by conductivity. For that reason our data are expressed in terms of the dielectric modulus, M^*, defined as the inverse of complex permittivity, ε^*, where $\varepsilon^* = \varepsilon' - i\varepsilon''$ and $M^* = M' - i'M''$ such that

$$M' + iM'' = (\varepsilon' - i\varepsilon'')^{-1} \tag{2}$$

resulting in

$$M' = \frac{\varepsilon'}{(\varepsilon')^2 + (\varepsilon'')^2} \quad \text{and} \quad M'' = \frac{\varepsilon''}{(\varepsilon')^2 + (\varepsilon'')^2} \tag{3}$$

The effect of temperature on the imaginary part of the dielectric modulus in the frequency domain is presented in Figure 2. The solid lines in the figure are fits to the HN functional form[31]

$$M^*(\omega) = \sum_{k=1}^{n} \left[\frac{\Delta M_k}{(1+(i\omega\tau_{Mk})^{a_k})^{b_k}} + M_{0k} \right] \tag{4}$$

Two relaxations are identified in this temperature range, and their locations are indicated by arrows in Figure 2. The segmental (α) process shifts to higher frequency and decreases in intensity with increasing temperature. The temperature dependence of the relaxation time for the α process is of the Vogel−Fulcher−Tammann (VFT) type

$$\tau = \tau_0 \exp\left(\frac{B}{T - T_V}\right) \tag{5}$$

Table 3. VFT Parameters for the Segmental Process

code	τ_0	B (K)	T_V (K)	T_g^{diel} (K)	$T_g^{Fox-Flory}$ (K)
D	1.0×10^{-14}	2408	210	275	
PEG-D18%	1.0×10^{-14}	4062	146	252	240
PEG-D10%	1.0×10^{-14}	3968	143	250	238
PEG-D5%	1.0×10^{-14}	3679	142	246	236
PEG	1.0×10^{-14}	3598	136	234	
PEGylated-8	1.0×10^{-14}	4422	253	273	
PEGylated-16	1.0×10^{-14}	4211	149	263	
PEGylated-32	1.0×10^{-14}	4177	146	260	

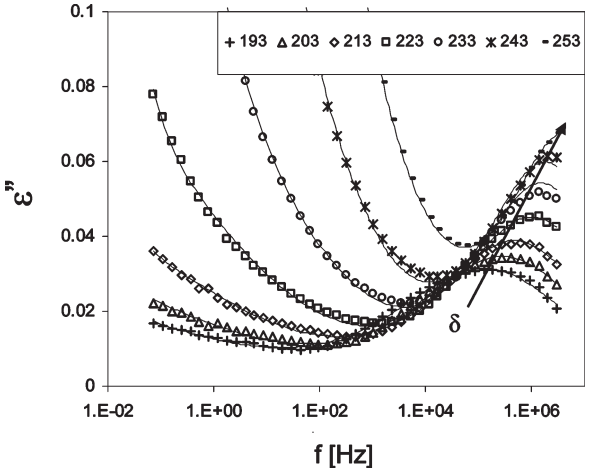

Figure 3. Dielectric loss of PEG in the frequency domain with temperature as a parameter.

where τ_0 refers to attempt frequency and T_V is the Vogel temperature which is usually 30−70 K below T_g. The corresponding VFT parameters are summarized in Table 3. The β process is seen at higher frequency.

B. Poly(ethylene glycol), PEG. PEG is a semicrystalline polymer with melting temperature of 327 K and degree of crystallinity, estimated from the heat of fusion, of 83%, regardless of the type of end group. Dielectric loss of PEG in the frequency domain, below 253 K with temperature as a parameter is presented in Figure 3. Above 253 K the spectra were dominated by conductivity, and these results are discussed below. PEG exhibits one relaxation in the temperature range between 193 and 253 K, termed δ, marked with an arrow in Figure 3. The δ process shifts to higher frequency, increases in intensity, and becomes narrower with increasing temperature. The temperature dependence of the relaxation time (τ_δ) is of the Arrhenius form with an activation energy of 22.5 kJ/mol. The low activation energy suggests that the origin of this process lies in the motion of local groups, most likely end groups.

At temperatures above 253 K, PEG spectra are presented in terms of the dielectric loss modulus as shown in Figure 4. One relaxation is identified and termed α_A. This relaxation has the characteristics of the segmental process within the amorphous phase. With increasing temperature the α_A process shifts to higher frequency and increases in intensity, in agreement with the previously reported characteristics of segmental motions in the amorphous phase of crystalline polymers.[32−35] The increase in the peak intensity persists up to 313 K. Above that temperature PEG melts and the intensity of the segmental process decreases. This is not surprising because it is known that the segmental process in fully amorphous systems decreases in intensity with increasing temperature. We acknowledge that the relaxation times obtained from the two formalisms, dielectric loss

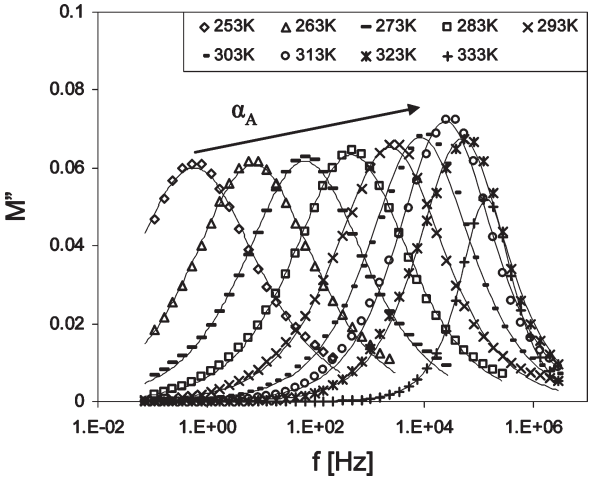

Figure 4. Dielectric loss modulus of PEG in the frequency domain with temperature as a parameter.

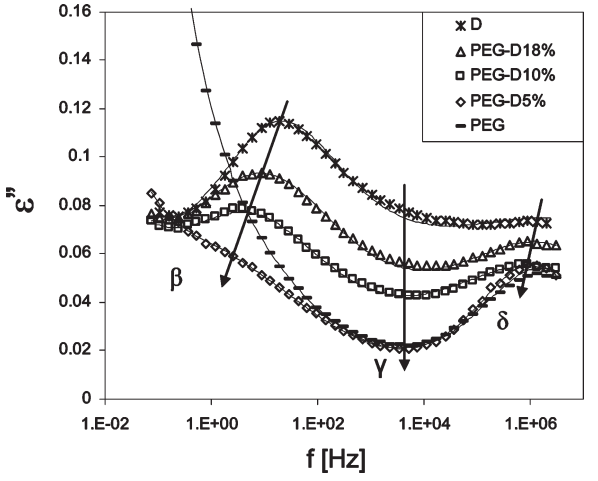

Figure 5. Dielectric loss of PEG−dendrimer blends in the frequency domain with dendrimer concentration as a parameter at 233 K.

modulus (τ_M) and dielectric loss (τ_ε), are not identical. However, their time scales are close,[35] and in the reminder of the text we shall refer to τ_M obtained from the HN fits of the dielectric modulus spectra as the average relaxation time. The relaxation time of the segmental process in the amorphous phase varies with temperature according to the VFT equation below T_m. Above T_m, however, the temperature dependence of the relaxation time assumes the Arrhenius form. We note that the investigated temperature range above T_m is narrow, making it difficult to distinguish between the Arrhenius and the VFT dependence.

2. Blends. We proceed with the analysis of blend dynamics. We build our discussion by focusing on the key parameters that define dynamics, namely the real and imaginary part of the dielectric permittivity, the shape of the relaxation spectra, the dielectric relaxation strength, the frequency location of the maximum loss, and the temperature dependence of the average relaxation time. First, we examine the relaxation dynamics of local processes and then proceed with the analysis of the segmental process. When dielectric loss is masked by conductivity, we use the dielectric modulus formalism.

2.1. Local Processes. Dendrimer concentration in the blend was varied between 5 and 18 wt % (Table1), and its effect on the dielectric loss in the frequency domain at 233 K is presented in Figure 5. Three processes similar to those observed in the individual components are present in the blends. The β and the γ process originate from the dendrimer, while the δ process represents a combination of the δ process in the dendrimer and PEG. Spectra generated at different temperatures below 253 K show the same trend in that the β and the δ process shift to lower frequency with decreasing dendrimers concentration. The γ process in the blends is present but is "hidden" in the frequency range between β and δ processes, as is the case in the neat dendrimer.

The spectral shape is described by the HN parameters a and b which define the breadth and the symmetry of the spectrum, respectively. The three local processes are symmetric in all blends ($b = 1$) and hence are well-described with the Cole−Cole equation.[30] The values of parameter a for the β and the δ process are summarized in Table 4. The β process becomes broader with increasing temperature, as in the neat dendrimer. It also becomes slightly broader with decreasing dendrimer concentration, although the reason for this behavior is not quite clear. The δ process becomes broader with

Table 4. Spectral Breadth Parameter as a Function of Temperature for Local Processes in PEG−Dendrimer Blends

		T [K]							
	code	173	183	193	203	213	223	233	243
β	D	0.50	0.50	0.50	0.50	0.50	0.48	0.47	0.45
	PEG-D18%	0.49	0.47	0.45	0.44	0.43	0.43	0.43	0.47
	PEG-D10%	0.46	0.45	0.44	0.43	0.43	0.43	0.42	0.42
	PEG-D5%			0.43	0.42	0.42	0.41	0.41	0.40
δ	D	0.28	0.29	0.30	0.30	0.30	0.30	0.32	0.36
	D18%-PEG	0.25	0.25	0.27	0.28	0.29	0.29	0.29	0.30
	D10%-PEG	0.27	0.28	0.28	0.29	0.31	0.33	0.36	0.39
	D5%-PEG			0.58	0.54	0.59	0.61	0.64	0.67

increasing dendrimer concentration because end groups on dendrimers and PEG experience a variety of local environments that become more complex with the addition of dendrimers. With increasing temperature, the δ process becomes broader, following the trend observed in the individual components. The parameter a for the γ process is independent of temperature and dendrimer concentration and is constant at 0.2. As in the neat dendrimer, the γ process is thermodielectrically simple, while the β and the δ process are thermodielectrically complex. This is intuitively expected because these processes originate from the same molecular motions as in the neat dendrimer and hence display analogous characteristics.

Dielectric relaxation strength ($\Delta\varepsilon$) of the local processes is examined next. This parameter is directly proportional to the concentration of dipoles and the mean-squared dipole moment per molecule and is defined by the relationship $\Delta\varepsilon = \varepsilon_0 - \varepsilon_\infty$, where ε_0 and ε_∞ represent the limiting low- and high-frequency dielectric permittivity, respectively. The effect of dendrimer concentration and temperature on the dielectric strength of blends was studied, and the results are plotted in Figure 6A for the β process and in Figure 6B for the δ process. An examination of the trends in $\Delta\varepsilon$ leads to the following principal observations: (1) $\Delta\varepsilon$ increases with increasing temperature for all three processes, which is a typical characteristic of a local process, and (2) $\Delta\varepsilon$ decreases with decreasing dendrimer concentration due to the decrease in the concentration of dipoles that contribute to these processes.

Next, we focus attention on the frequency location of the maximum loss and its temperature dependence. Figure 7 shows the average relaxation time as a function of temperature for the β process (A) and the δ process (B), obtained

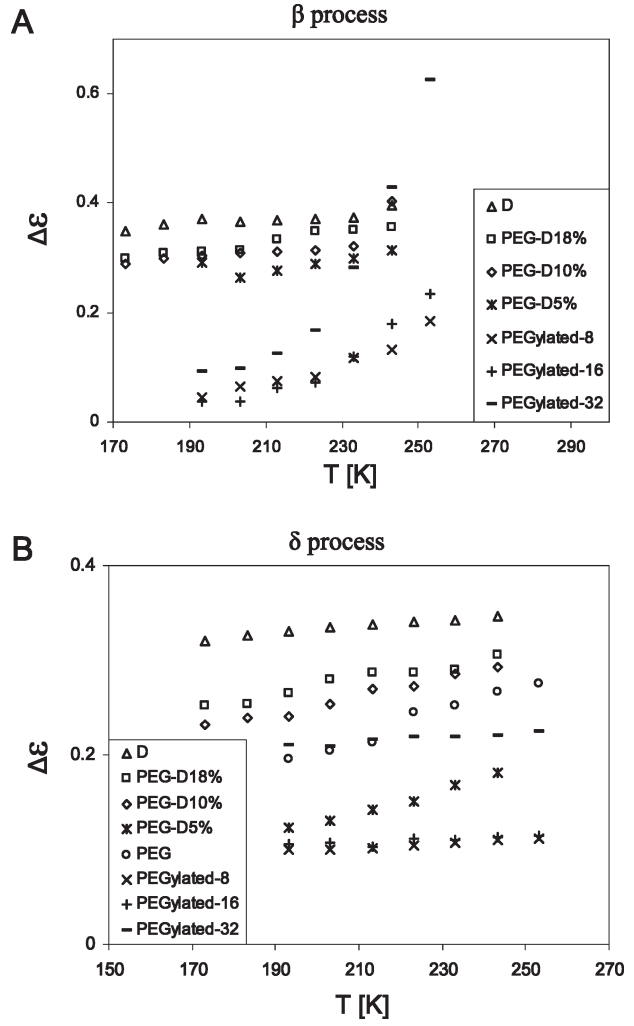

Figure 6. Dielectric relaxation strength as a function of temperature with dendrimer concentration as a parameter for PEG−dendrimer blends and the average number of attached PEG chains as a parameter for PEGylated dendrimers for (A) the β process and (B) the δ process.

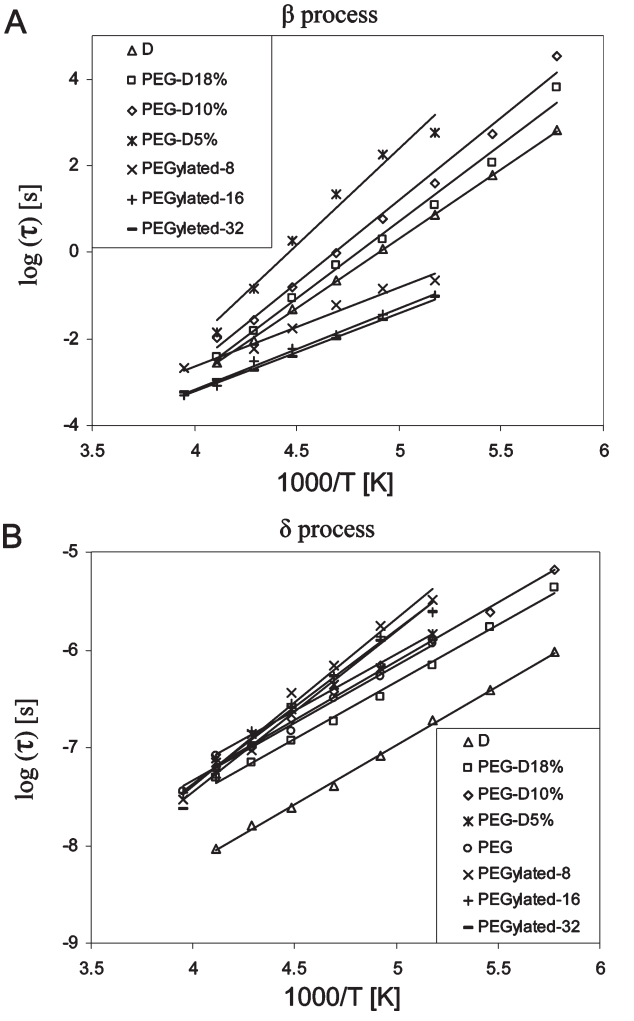

Figure 7. Average relaxation time as a function of reciprocal temperature for PEG−dendrimer blends and PEGylated dendrimers for (A) the β process and (B) the δ process.

from the HN fits. The solid lines are the Arrhenius fits. The activation energy for the β process varies as follows: 61.5 kJ/mol for D, 68.0 kJ/mol for PEG-D18%, 73.1 kJ/mol for PEG-D10%, and 90.8 kJ/mol for PEG-D5%. Note that the activation energy for this process increases with decreasing dendrimer concentration. The calculated values of the activation energy for the δ process are 23.4 kJ/mol for D, 22.4 kJ/mol for PEG-D18%, 23.0 kJ/mol for PEG-D10%, and 24.0 kJ/mol for PEG-D5%. Activation energy for this process is not a function of dendrimer concentration. However, both processes slow down with decreasing dendrimer concentration (see Figure 5), and we believe that this results from the H-bonding between PEG oxygen and amino groups on the dendrimer surface, which are involved in both β and δ relaxation.

2.2. Segmental Process. Dielectric loss for blends in the temperature range where the segmental process occurs is masked by conductivity. Therefore, our data are expressed in terms of dielectric modulus. Figure 8 shows dielectric modulus in the frequency domain with dendrimer concentration as a parameter, at 293 K. Real and loss modulus data are plotted in parts A and B of Figure 8, respectively. Note how loss modulus peak increases in intensity and shifts to higher frequency with decreasing dendrimer concentration. This is an interesting observation, and we will revert to it shortly. The solid lines are fits to the HN form (eq 4). An examination of the HN parameters a and b shows that the segmental process becomes more asymmetric with increasing temperature. This is not surprising because the same behavior is observed in the neat dendrimer. The segmental process also becomes more asymmetric with increasing dendrimer concentration. Spectral breadth, on the other hand, first increases and then decreases with increasing temperature. The reason is that this process is dominated by segmental relaxation in dendrimers at lower and PEG at higher temperature. An increase in dendrimer concentration also results in spectral broadening. This is because segmental reorientations occur with different rates in variety of environments that are rendered more complex with the addition of dendrimers.

The dielectric modulus strength (ΔM), defined as $\Delta M = M_\infty - M_0$, is proportional to the dielectric strength ($\Delta\varepsilon$) and is calculated using $M_0 = 1/\varepsilon_0$ and $M_\infty = 1/\varepsilon_\infty$, as defined by Wagner and Richert.[36] Dielectric modulus strength for the α process (ΔM_α) varies with temperature as shown in Figure 9. This figure also contains the data for PEGylated dendrimers, which are discussed later. Four principal findings for the blends are (1) ΔM_α shows discontinuity at the melting temperature, (2) at a given concentration, ΔM_α is not a function of temperature, (3) ΔM_α increases with decreasing dendrimer concentration below T_m, and (4) ΔM_α decreases with decreasing dendrimer concentration above T_m.

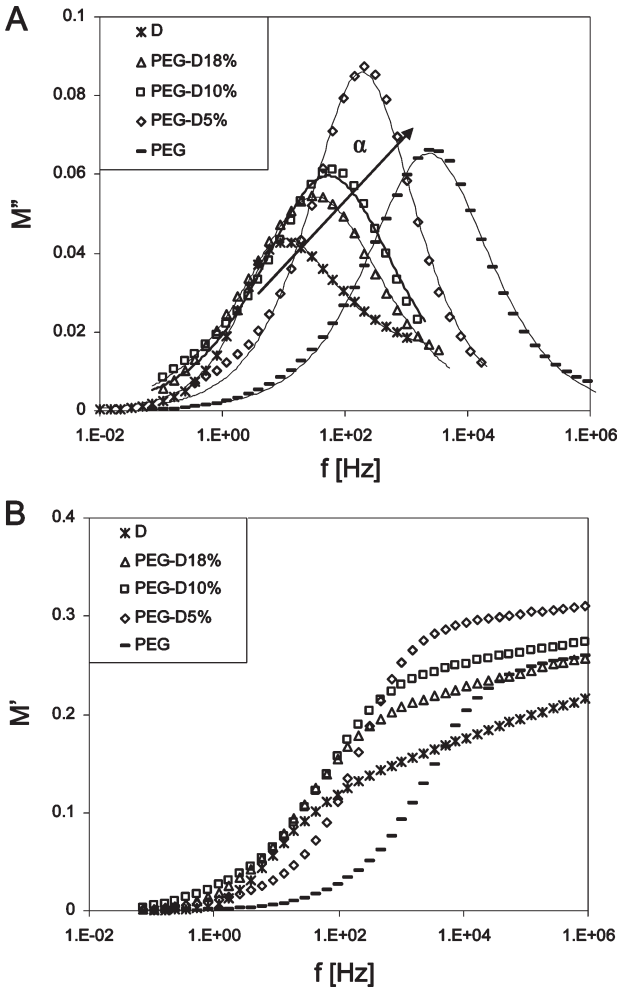

Figure 8. Dielectric modulus (A, loss part; B, real part) in the frequency domain with dendrimer concentration as a parameter for PEG−dendrimer blends at 293 K.

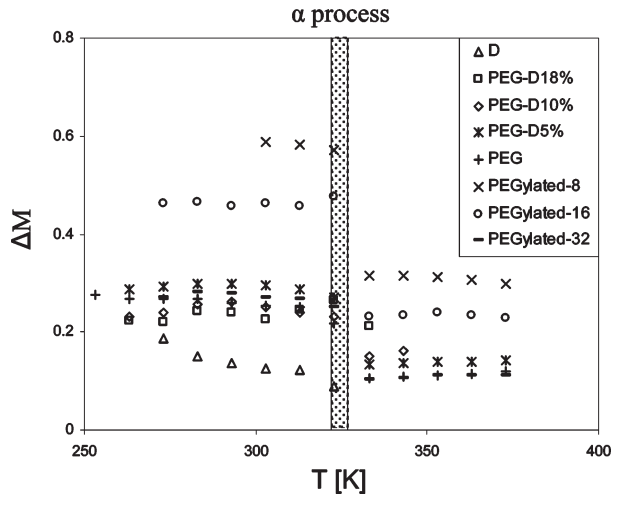

Figure 9. Dielectric modulus strength as a function of temperature with dendrimer concentration as a parameter for PEG−dendrimer blends and the average number of attached PEG chains as a parameter for PEGylated dendrimers for the α process. The dimmed rectangle represents the melting region.

The average relaxation time for the α process was examined next and is presented as a function of reciprocal temperature in Figure 10. Two regions are readily identified

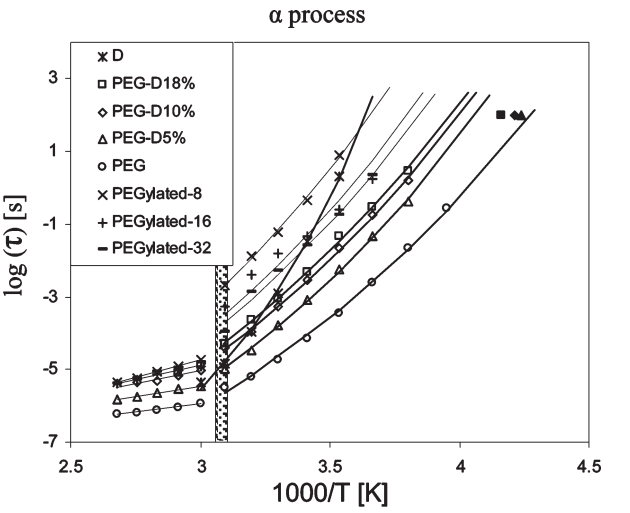

Figure 10. Average relaxation time as a function of reciprocal temperature for PEG−dendrimer blends and PEGylated dendrimers for the α process. The solid symbols represent glass transition temperature calculated using the Fox−Flory equation. The dimmed rectangle corresponds to the melting region.

in this figure and are divided by the dimmed rectangle which encompasses the melting region. Above T_m the data follow Arrhenius behavior. Below T_m the VFT behavior is observed. The solid lines to the right of the melting region are the VFT fits, and we note a very good agreement between the data and the results of regression analysis. The corresponding VFT parameters are summarized in Table 3. This table also contains the operational values of the "dielectric glass transition" temperature defined as the temperature where τ_α equals 100 s. The glass transition temperature was also calculated using the Fox−Flory equation:[37]

$$T_g = \frac{T_{g_1} T_{g_2}}{w_1 T_{g_2} + w_2 T_{g_1}} \quad (6)$$

where T_{g_1} and T_{g_2} are the glass transition temperatures of blend components and w_1 and w_2 their weight percent in the blend. These temperatures are also included in Figure 10 as filled symbols (upper right corner). "Dielectric glass transition" temperatures are, on average, about 11 K higher than the values obtained from the Fox−Flory equation. The observed increase in the time scale of the segmental process in blends in comparison with PEG is attributed to the restriction of mobility caused by the H-bonding between dendrimers and PEG.

3. PEGylated Dendrimers. PEGylated dendrimers are produced by chemical reaction between the functional end group on the dendrimer (amine) and the functional end group on PEG (epoxy), according to the following well-known reaction:[25]

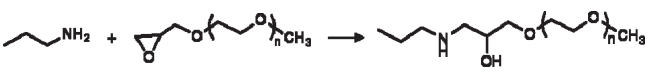

In the text below, we describe the results for local and segmental relaxation in terms of key dynamic parameters.

3.1. Local Processes. Figure 11 shows dielectric loss in the frequency domain for PEGylated dendrimers at 233 K with the average number of attached PEG chains (8, 16, or 32) as a parameter. All PEGylated dendrimers are characterized by two local relaxations, termed β and δ. Both processes shift to

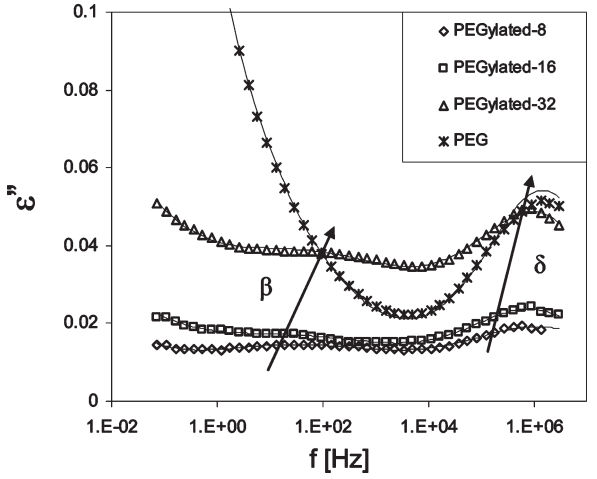

Figure 11. Dielectric loss in the frequency domain with average number of attached PEG chains as a parameter for PEGylated dendrimers at 233 K.

Table 5. Spectral Breadth Parameter as a Function of Temperature for Local Processes in PEGylated Dendrimers

		T [K]						
	code	193	203	213	223	233	243	253
B	PEGylated-8	0.39	0.37	0.33	0.34	0.28	0.28	0.24
	PEGylated-16	0.50	0.49	0.35	0.34	0.28	0.24	0.24
	PEGylated-32	0.44	0.43	0.38	0.34	0.27	0.24	0.21
	PEG							
Δ	PEGylated-8	0.36	0.38	0.40	0.42	0.45	0.47	0.48
	PEGylated-16	0.37	0.39	0.43	0.43	0.46	0.47	0.47
	PEGylated-32	0.34	0.34	0.35	0.36	0.39	0.39	0.38
	PEG	0.38	0.40	0.43	0.44	0.50	0.52	0.55

higher frequency and increase in intensity with increasing temperature. The δ process in PEGylated dendrimers is related to the δ process in the neat PEG and dendrimers, whose molecular origin was attributed to the motions of end groups. This process increases in intensity and shifts to higher frequency with increasing amount of PEG. The β process in PEGylated dendrimers, however, is a new process that is not observed in the neat dendrimer or neat PEG and is a consequence of the formation of covalent bonds between the reactive functional groups on dendrimers and PEG. This process increases in intensity and shifts to higher frequency with an increase in the average number of attached PEG chains. At present, however, the precise molecular origin of this process is not completely clear.

The HN fits of dielectric spectra show that both β and δ relaxations are symmetric. With increasing temperature, the HN breadth parameter decreases for the β process and, as in the neat PEG, increases for the δ process (see Table 5).

Dielectric relaxation strength of each process is shown in Figure 6. Dielectric relaxation strength for the β process ($\Delta\varepsilon_\beta$) and the δ process ($\Delta\varepsilon_\delta$) increase with increasing temperature by 6 and 1.1, respectively. Both $\Delta\varepsilon_\beta$ and $\Delta\varepsilon_\delta$ also increase with increasing amount of PEG, as a result of the increasing concentration of dipoles that contribute to these processes.

The average relaxation time for the β process and the δ process, shown in Figure 7, follows the Arrhenius form, and the calculated activation energies are summarized in Table 2.

3.2. Segmental Process. The dielectric modulus formalism was employed to identify the segmental process in PEGylated dendrimers. The effect of the average number of PEG chains attached to the dendrimer on the imaginary and real

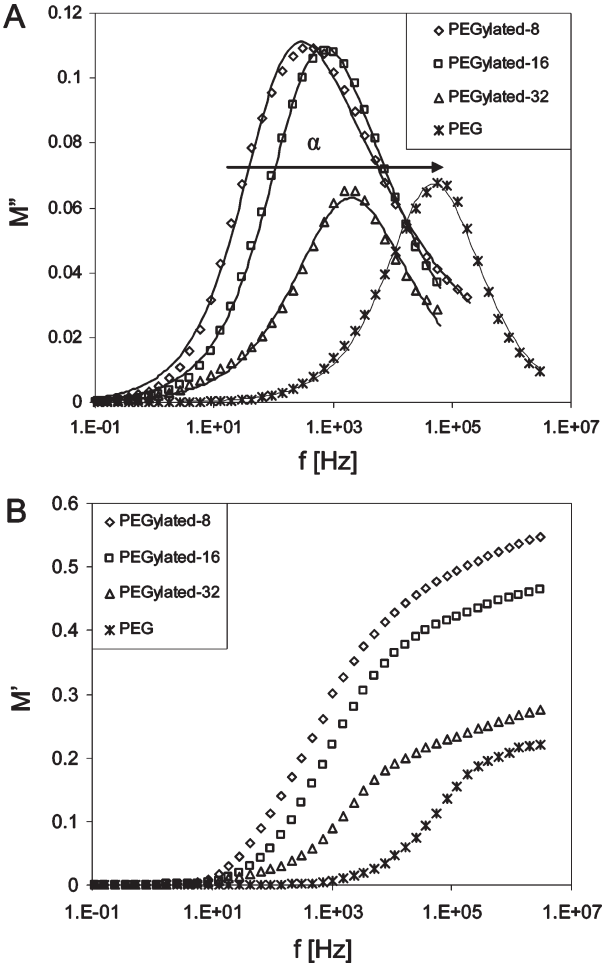

Figure 12. Dielectric modulus (A, loss part; B, real part) in the frequency domain with average number of attached PEG chains as a parameter for PEGylated dendrimers at 323 K.

part of the dielectric modulus in the frequency domain is presented in parts A and B of Figure 12, respectively. The time scale of the segmental process decreases by 1 order of magnitude in going from PEGylated-8 to PEGylated-32, while the intensity decreases with increasing PEG content. The HN fits reveal an asymmetric segmental process in the temperature range from 273 to 373 K, with the HN parameter b increasing in the range 0.34−0.61 as a function of decreasing temperature. The temperature dependence of parameter a is different below and above T_m: (1) below T_m the spectra become narrower with increasing temperature (a increases from 0.62 to 0.91), which is in agreement with previously observed characteristics for the segmental process in the amorphous phase,[33−35] and (2) above T_m parameter a is independent of temperature and equal to 1. At any temperature, an increase in the average number of attached PEG chains leads to spectral broadening. This broadening is a direct consequence of the increase in crystallinity with increasing amount of PEG (see Table 1). Similar results were reported for other semicrystalline polymers.[38−42]

Figure 9 shows the dependence of ΔM on temperature and the number of attached PEG chains. ΔM is independent of temperature below T_m, undergoes a step change at T_m, and drops to another constant value above T_m. Further, ΔM decreases with an increasing number of attached PEG chains both below and above T_m. Below T_m, the degree of crystallinity of the complex increases with increasing amount of PEG, and consequently, the number of dipoles that

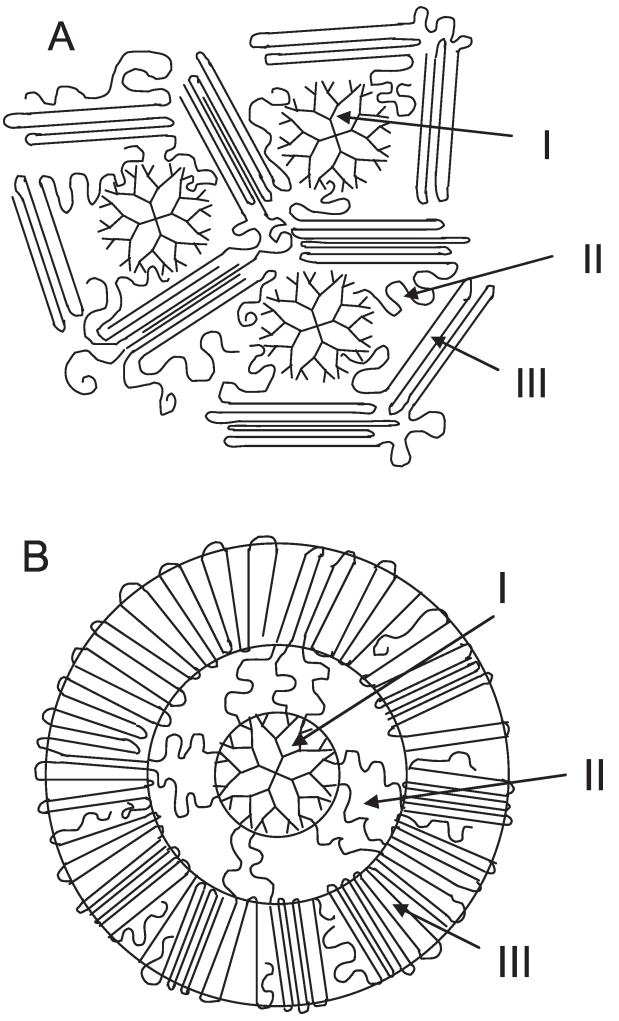

Figure 13. Schematic of the proposed morphology: I, dendrimer; II, amorphous PEG; and III, crystalline phase in (A) PEG−dendrimer blends and (B) PEGylated dendrimers.

contribute to the segmental process in the amorphous phase decreases.

The average relaxation time (τ_M) obtained from the HN fits is included in the composite plot in Figure 10. The data below T_m are fitted to the VFT equation, and the corresponding parameters are listed in Table 3. In the narrow temperature range above T_m the data are well described by the Arrhenius equation.

One very interesting observation is the difference in the temperature dependence of the average relaxation time for the PEG−dendrimer blends and the PEGylated dendrimers. In the blends, the extrapolation of the VFT behavior from the low temperature coincides at the melting point with the extrapolation of the Arrhenius behavior from the high temperature. In the PEGylated dendrimers, however, we observe a discontinuity at the melting point as the time scale of relaxation decreases dramatically in the melt (by ca. 2 decades on the log(τ) scale). Another interesting finding regards the α_A process above T_m in that the relaxation time of the α_A process is a function of dendrimer concentration in the blend but is independent of the average number of attached PEG chains in PEGylated dendrimers. An explanation of this phenomenon is offered below in terms of the difference in the morphology of blends and PEGylated dendrimers.

Our concept of morphology is shown schematically in Figure 13 for PEG−dendrimer blends (Figure 13A) and PEGylated dendrimers (Figure 13B). The proposed morphology is based on the observed dielectric relaxation phenomena and previous reports.[28,43] The noncrystalline regions in both systems contain dendrimers (I) and the amorphous phase of PEG (II), while the crystalline portion consists of the PEG lamellae (III).[43] The origin of α relaxation in PEG−dendrimer blends and in PEGylated dendrimers is common: it lies in the motions within the amorphous phase of PEG. But there are two principal differences. First, H-bonds are plentiful in blends but are present to a lesser extent in PEGylated dendrimers due to the different morphology. Second, we believe the amorphous PEG in the blends is constrained by the covalent bond to the crystalline lamellae only. In PEGylated dendrimers, however, the amorphous PEG is doubly confined: by the crystalline lamellae on the one side and the covalent bonds to the dendrimer on the other. As a consequence, the relaxation in PEGylated dendrimers has a longer time scale than in blends.

Finally, the time scale of segmental relaxation in PEGylated dendrimers below T_m increases with decreasing number of attached PEG chains. This appears to be a direct consequence of the decrease in crystallinity with decreasing amount of PEG. Above T_m, however, the movements of PEG chains are not restricted anymore by crystals, and consequently the average relaxation time is independent of the number of attached PEG chains. But in the blends, H-bonds form below as well as above T_m, and thus the average relaxation time remains a function of dendrimer concentration over the entire temperature range.

Conclusions

We have completed an investigation of the dynamics of a series of PEG−dendrimer blends and PEGylated dendrimers. The effect of temperature, dendrimer concentration, and the average number of attached PEG chains on various relaxation processes was probed by dielectric relaxation spectroscopy (DRS) over the frequency range from 10^{-1} to 10^6 Hz and at temperatures from 193 to 373 K. The principal conclusions are as follows.

In PEG−dendrimer blends, three local processes are identified and defined as β, γ, and δ in the order of increasing frequency at a constant temperature. The β and the γ process originate from the dendrimer, while the δ process represents a combination of the δ process in the dendrimer and PEG. All three processes are characterized by symmetric, Cole−Cole type relaxation spectra and an Arrhenius-like temperature dependence of the average relaxation time. The β and the δ process slows down with decreasing dendrimer concentration due to the H-bonding that forms between PEG oxygen and amino groups on the dendrimer surface. Dielectric modulus formalism was used to identify the segmental process in the blends. The time scale of the segmental process increases with increasing dendrimer concentration. The observed increase in the time scale is attributed to the restriction of mobility caused by the H-bonding between dendrimers and PEG.

PEGylated dendrimers are characterized by two local relaxation processes. The faster process is related to the δ process in the neat PEG, whose molecular origin was attributed to the motions of end groups. The slower one, however, is a new process that is not present in the neat dendrimers or PEG and is a consequence of the formation of covalent bonds between the reactive functional groups. The α process was identified using dielectric modulus formalism and associated with the motions within the amorphous phase of PEG.

There are two principal differences in morphology between blends and PEGylated dendrimers: (1) H-bonds are abundant in blends but scarce in PEGylated dendrimers, and (2) amorphous

PEG in the blends is covalently constrained by the crystalline lamellae only, while in PEGylated dendrimers it is doubly confined: by the crystalline lamellae on the one side and the covalent bonds to the dendrimer on the other. As a consequence, the time scale of α relaxation in PEGylated dendrimers is longer than in blends.

Acknowledgment. This material is based on work supported by National Science Foundation under Grant DMR-0346435.

References and Notes

(1) Langer, R. *Science* **1990**, *249*, 1527.
(2) Kathryn, E. U.; Scott, M. C.; Robert, S. L.; Kevin, M. S. *Chem. Rev*. **1999**, *99*, 3181.
(3) Kataoka, K.; Harada, A.; Nagasaki, Y. *Adv. Drug Delivery Rev*. **2001**, *47*, 113.
(4) Duncan, R. *Nat. Rev. Drug Discovery* **2003**, *2*, 347.
(5) Esfand, R.; Tomalia, D. A. *Drug Discovery Today* **2001**, *6*, 427.
(6) Calabretta, M. K.; Kumar, A.; McDermott, A. M.; Cai, C. *Biomacromolecules* **2007**, *8*, 1807.
(7) Patri, A. K.; Majoros, I. J.; Baker, J. R.Jr. *Curr. Opin. Chem. Biol*. **2002**, *6*, 466.
(8) Gupta, U.; Agashe, H. B.; Asthana, A.; Jain, N. K. *Biomacromolecules* **2006**, *7*, 649.
(9) Gillies, E. R.; Frèchet, J. M. J. *Drug Discovery Today* **2005**, *10*, 35.
(10) Majoros, I. J.; Myc, A.; Thomas, T.; Chandan, B. M.; Baker, J. R. Jr. *Biomacromolecules* **2006**, *7*, 572.
(11) Boas, U.; Heegaard, P. M. H. *Chem. Soc. Rev*. **2004**, *33*, 43.
(12) Torchilin, V. P., Ed. *Nanoparticulates as Drug Carriers*; Imperial College Press: London, England, 2006.
(13) Frechet, J. M. J.; Tomalia, D. A. *Dendrimers and Other Dendritic Polymers*; Wiley: West Sussex, England, 2001.
(14) Newkome, G. R.; Moorefield, C. N.; Vogtle, F. *Dendrimers and Dendrons: Concept, Synthesis, Applications*; Wiley-VCH: Weinheim, 2001.
(15) Bosman, A. W.; Janssen, H. M.; Meijer, E. W. *Chem. Rev*. **1999**, *99*, 1665.
(16) Kallos, G. J.; Tomalia, D. A.; Hedstrand, D. M.; Lewis, S.; Zhou, J. *Rapid Commun. Mass Spectrom*. **1991**, *5*, 383.
(17) Zhou, J.; Wu, J.; Hafdi, N.; Behr, J. P.; Erbacher, P.; Peng, L. J. *Chem. Commun*. **2006**, 2362.
(18) Roberts, J. C.; Bhalgat, M. K.; Zera, R. T. *J. Biomed. Mater. Res*. **1996**, *30*, 53.
(19) Jevprasesphant, R.; Penny, J.; Jalal, R.; Attwood, D.; McKeown, N. B.; D'Emanuele, A. *Pharm. Res*. **2003**, *20*, 1543.
(20) Kobayashi, H.; Kawamoto, S.; Saga, T.; Sato, N.; Hiraga, A.; Ishimori, T.; Konishi, J.; Togashi, K.; Brechbiel, M. W. *Magn. Reson. Med*. **2001**, *46*, 781.
(21) Bhadra, D.; Bharda, S.; Jain, S.; Jain, N. K. *Int. J. Pharm*. **2003**, *257*, 111.
(22) Williams, G. Dielectric relaxation spectroscopy of amorphous polymer systems. The modern approach. In *Keynote Lectures in Polymer Science*; Riande, E., Ed.; CSIC: Madrid, 1995.
(23) Riande, E.; Diaz-Calleja, R. *Electrical Properties of Polymers*; Marcel Dekker: New York, 2004.
(24) Kremer, F., Schonhals, A., Eds. *Broadband Dielectric Spectroscopy*; Springer-Verlag: Berlin, 2002.
(25) Fitz, B.; Andjelic, S.; Mijovic, J. *Macromolecules* **1997**, *30*, 5227.
(26) Mijovic, J.; Andjelic, S. *Macromolecules* **1996**, *29*, 239.
(27) Mijovic, J.; Ristic, S.; Kenny, J. *Macromolecules* **2007**, *40*, 5212.
(28) Ristic, S.; Mijovic, J. *Polymer* **2008**, *49*, 4695.
(29) Havriliak, S. J.; Negami, S. *Polymer* **1967**, *8*, 161.
(30) Cole, R. H.; Cole, K. S. *J. Chem. Phys*. **1942**, *10*, 98.
(31) Sun, M.; Pejanovic, S.; Mijovic, J. *Macromolecules* **2005**, *38*, 9854.
(32) Huo, P.; Cebe, P. *Macromolecules* **1992**, *25*, 902.
(33) Williams, G. Electric Phenomenon in Polymer Science. In *Molecular Aspects of Multiple Dielectric Relaxation Processes in Solid Polymers*; Springer: Berlin, 1979.
(34) Sy, J. W.; Mijovic, J. *Macromolecules* **2000**, *33*, 933.
(35) Mijovic, J.; Sy, J. W.; Kwei, T. K. *Macromolecules* **1997**, *30*, 3042.
(36) Wagner, H.; Richert, R. *Polymer* **1997**, *38*, 255.
(37) Fox, T. G.; Flory, P. J. *J. Am. Chem. Soc*. **1948**, *70*, 2384.
(38) Sasabe, H.; Saito, S.; Asahina, M.; Kakutari, H. *J. Polym. Sci*. **1960**, *27*, 1405.
(39) Boyd, R. H. *Polymer* **1985**, *26*, 323.
(40) Ishida, Y.; Yamafuji, K.; Itch, H.; Takayanagi, H.; Kolloid, Z. Z. *Polymer* **1962**, *184*, 97.
(41) Dobbertin, J.; Hensel, A.; Schick, C. *J. Therm. Anal*. **1996**, *47*, 1027.
(42) Natesan, B.; Hui, X.; Ince, B. S.; Cebe, P. *J. Polym. Sci., Part B: Polym. Phys*. **2004**, *42*, 777.
(43) Johnson, M. A.; Iyer, J.; Hammond, P. T. *Macromolecules* **2004**, *37*, 2490.